Electronically Tuned Local Oscillators for the NOEMA Interferometer

Francois Mattiocco, *Member, IEEE*, Olivier Garnier, Doris Maier, Alessandro Navarrini, and Patrice Serres

***Abstract*—We present an overview of the electronically tuned local oscillator (LO) system developed at the Institut de RadioAstronomie millimetrique (IRAM) for the superconductor–insulator–superconductor (SIS) receivers of the NOrthern Extended Millimeter Array interferometer (NOEMA). We modified the frequency bands and extended the bandwidths of the LO designs developed by the National Radio Astronomy Observatory (NRAO) for the Atacama Large Millimeter Array (ALMA) project to cover the four NOEMA LO frequency ranges 82–108.3 GHz (Band 1), 138.6–171.3 GHz (Band 2), 207.7–264.4 GHz (Band 3), and 283–365 GHz (Band 4). The NOEMA LO system employs commercially available MMICs and GaAs millimeter MMICs from NRAO which are micro-assembled into active multiplied chain (AMC) and power amplifier (PA) modules. We discuss the problem of the LO spurious harmonics and of the LO signal directly multiplied by the SIS mixers that add extra noise and lead to detections of unwanted spectral lines from higher order sidebands. A waveguide filter in the LO path is used to reduce the higher order harmonics level of the LO at the output of the final frequency multiplier, thus mitigating the undesired effects and improving the system noise temperature.**

***Index Terms*—Electronically tuned local oscillators, interferometry, MMIC, MVNA, passband filter, waveguide coupler, YIG.**

I. Introduction

FOR many years, the wideband millimeter-wave heterodyne SIS receivers installed on the six 15-m-diameter antennas of the IRAM Plateau de Bure Interferometer (PdBI) have employed local oscillator (LO) systems based on commercial solid-state Gunn local oscillators [1]. The Gunn oscillators for Band 1 operate across $\sim$ 82–116 GHz, while those for Bands 2 and 3 operate across $\sim$ 67–90 GHz and are cascaded with frequency multipliers[1] (a doubler for Band 2 and a tripler for Band 3) in order to generate the final LO frequency. The Gunn LO systems have proved to perform reliably on-site. However, the tuning of the oscillators by two motorized mechanical backshorts is time-consuming and not perfectly reproducible. Thus, with the advent of the NOrthern Extended Millimeter Array interferometer (NOEMA), we decided to replace the Gunn LO systems with new electronically tuned LO systems. The NOEMA project aims at upgrading the PdBI interferometer from six to 12 antennas equipped with new dual-polarization quad-band sideband separating (2SB) SIS receivers delivering four $\sim$ 3.8–11.6-GHz IF bands. As part of this project, we extended, with some modifications, the LO design developed by the NRAO [2], [3] for the ALMA project to the four NOEMA frequency bands. In particular, after design adaptation, we built and tested: 1) eight (seven plus one spare) 283–365-GHz electronically tuned LO systems for NOEMA Band 4 (similar to the ALMA Band 7 LO), six of which have been in use in the six PdBI antennas since 2010 and 2) five (four plus one spare) 82–108.3-GHz electronically tuned LO system for NOEMA Band 1, of which the prototype has been in use on the first new NOEMA antenna, Ant. #7 since December 2014. The Gunn oscillator systems that have been in use on Bands 2 and 3 will be maintained on the NOEMA antennas. However, an electronically tuned LO prototype has been designed to cover simultaneously the NOEMA Bands 2&3 associated with a mm-wave switch that selects either a doubler (Band 2) or a tripler (Band 3).

Here, we present the design features of the NOEMA LO system, which we also discussed in [4], by pointing out the main differences with respect to the NRAO LO systems developed for ALMA. The performances in the different NOEMA LO bands will be presented. Also, we will discuss our measurement results of the spurious harmonics content of the LO system and the adopted solution to reject such harmonics using a wideband waveguide filter.

II. NOEMA LO System

A synoptic diagram for the four bands of the future NOEMA LO system is shown in Fig. 1. Three independent commercial Yttrium Iron Garnet (YIG) oscillators (MLXS-1783, MLXS-1795 and MLOS-1604) [5] are used: 1) one covering 12.86–19.53 GHz for Band 1 (82–108 GHz); 2) one covering 11–15 GHz for Band 2 (138.6–171.3 GHz) and Band 3 (207.74–264.38 GHz), which will share this common drive oscillator; and 3) one covering 15–21 GHz for Band 4 (283–365 GHz). Each YIG oscillator drives an active multiplied chain (AMC) module, which is cascaded with a power amplifier (PA). Band 1 uses a single AMC module named AMC1, Band 2&3 and Band 4 use an AMC module followed by a PA module and a 3-dB recombination hybrid coupler. Bands 2 and 3 use the same AMC2–3 and PA2–3 modules. The output of the common Bands 2 and 3 module is connected to a mechanical switch, which diverts the LO signal to either a frequency doubler for Band 2 or to a frequency tripler for Band 3. The nonswitched position of the switch is terminated with a waveguide load that absorbs the LO power of the unselected

Manuscript received November 18, 2015 revised November 18, 2015; accepted January 18, 2016. *(Corresponding author: Francois Mattiocco.)*

The authors are with the Institut de Radio Astronomie Millimétrique (IRAM), 38406 Saint Martin d'Hères, France (e-mail: mattiocc@iram.fr).

Color versions of one or more of the figures in this paper are available online at http://ieeexplore.ieee.org.

Digital Object Identifier 10.1109/TTHZ.2016.2525813

[1][Online]. Available: www.vadiodes.com

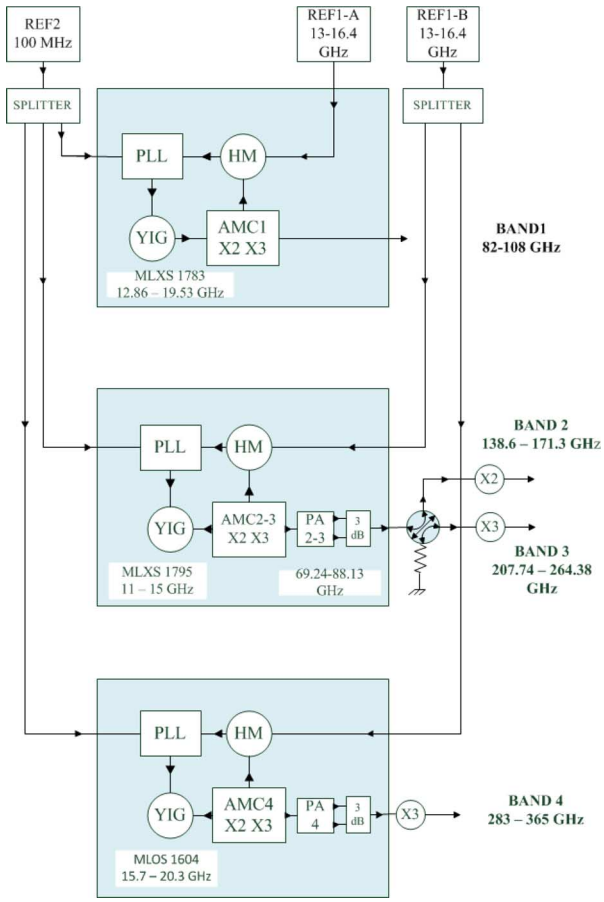

Fig. 1. Synoptic diagram of future all-electronically tunable LO system for the NOEMA interferometer consisting of three racks. In Band 1, the YIG oscillator drives an active multiplied chain (AMC1), while in Bands 2 and 3 a single YIG oscillator drives a common AMC (AMC2–3) which is cascaded with a PA (PA2–3) whose output is diverted by a switch to either a frequency doubler (Band 2) or frequency tripler (Band 3). In Band 4, the YIG oscillator drives the AMC4, which is cascaded with the PA4 that feeds a final frequency tripler. The 3-dB hybrid couplers are cascaded with PA2–3 and PA4.

band. The Band-1 LO will operate continuously by means of a dedicated YIG oscillator and a dedicated reference so that it will always be available for dual frequency calibration purposes.

Two first phase-locked loop (PLL) reference signals (REF1, 13–16.4 GHz) from two independent modules employing four output connectors are available in the system. One module provides the first reference for Band 1, while the second module provides the reference for Band 2&3 and for Band 4. The second PLL reference (REF2, 100 MHz) is distributed between all PLLs through a splitter. All LOs are locked with the REF2 signal using a harmonic mixer (HM) that is coupled with the AMC module and pumped by REF1. The 100-MHz IF from the harmonic mixer is filtered and amplified before entering the 100-MHz PLL box. A CAN interface controls the YIG PLL as well as the AMC and PA bias, which allows to regulate the power available at the LO system output.

The signals at the output of the three NOEMA LO racks (represented by the three largest boxes in the diagram of Fig. 1) are sent through three independent waveguides to the backplate of the NOEMA Front-End cryostat where the final frequency multipliers and the waveguide switch are located. After frequency multiplication, the LO signals run inside the cryostat through four waveguides (overmoded in the three higher bands) down to four independent waveguide splitters (one per band), each dividing the LO between the two sideband separating SIS mixers of the two independent polarization channels (two 2SB mixers per band, i.e., eight mixers in total). The LO splitters and SIS mixers are in thermal contact with the 4 K stage of the cryostat.

III. LO Design

The architecture of the AMC and PA Monolithic Microwave Integrated Circuit (MMIC) micro-assembly is very similar for all four NOEMA bands, and only the Band-1 modules are presented here. The Band-1 PA (PA1) and 3-dB coupler modules will find application in a LO system for a future 3-mm multibeam receiver, but they are not used in the NOEMA Band-1 LO system described in this paper.

A. AMC and PA

Here, we present the details of the AMC, PA, and 3-dB coupler modules with base specifications taken from the initial LO Band-1 design ($\sim$ 85.7–108.2 GHz;see Fig. 2). The measurement results proved that the LO Band-1 system worked very well and that even the more extended goal bandwidth, 80–108 GHz, could be achieved, as discussed in Section VI. In Fig. 2, the PA and the 3-dB coupler modules are presented in upside-down orientation compared with the AMC in order to show more clearly the details of the MMICs packaging. A photograph of the fabricated and assembled AMC1 module is shown in Fig. 3.

The three modules (AMC, PA, and 3-dB coupler) are aligned with dowel pins, assembled with M2.5 screws, and arranged inside a 19-in 4U rack together with other electronics components (described below).

In the AMC1, the 14.29–18.04-GHz input signal coming from the YIG oscillator goes through a 28.58–36.08 GHz MMIC frequency doubler (HMC578), a MMIC amplifier (AMMC5040), a band pass filter, and a MMIC frequency tripler [9] (the desired AMC output signal frequency is 6 times the AMC input frequency). At the tripler output, the 85.744–108.256 GHz signal is amplified by a medium power MMIC amplifier [3] and filtered by a pass-band filter. Then a waveguide-to-microstrip line transition couples the LO signal into a long WR10 waveguide that carries the signal to the output of the AMC. A fraction of the multiplied LO signal (-10 dB) is coupled to a PLL harmonic mixer located outside the AMC module, marked as PLL output in Fig. 2.

The AMC waveguide output is connected to the waveguide input of the PA inside which the main LO output signal is amplified using a balanced scheme with a 3-dB hybrid coupler, two medium-power MMIC amplifiers [3] and an additional 3-dB coupler that combines the two amplified signals inside a separate mechanical module. The use of the 3-dB hybrid coupler optimizes the saturated power level and the output return loss.

The NOEMA LO design includes the following modifications relative to the ALMA LO design.

- Filters and waveguide transitions have been redesigned for different frequency bands with larger relative bandwidth than in ALMA, except for Band 4.

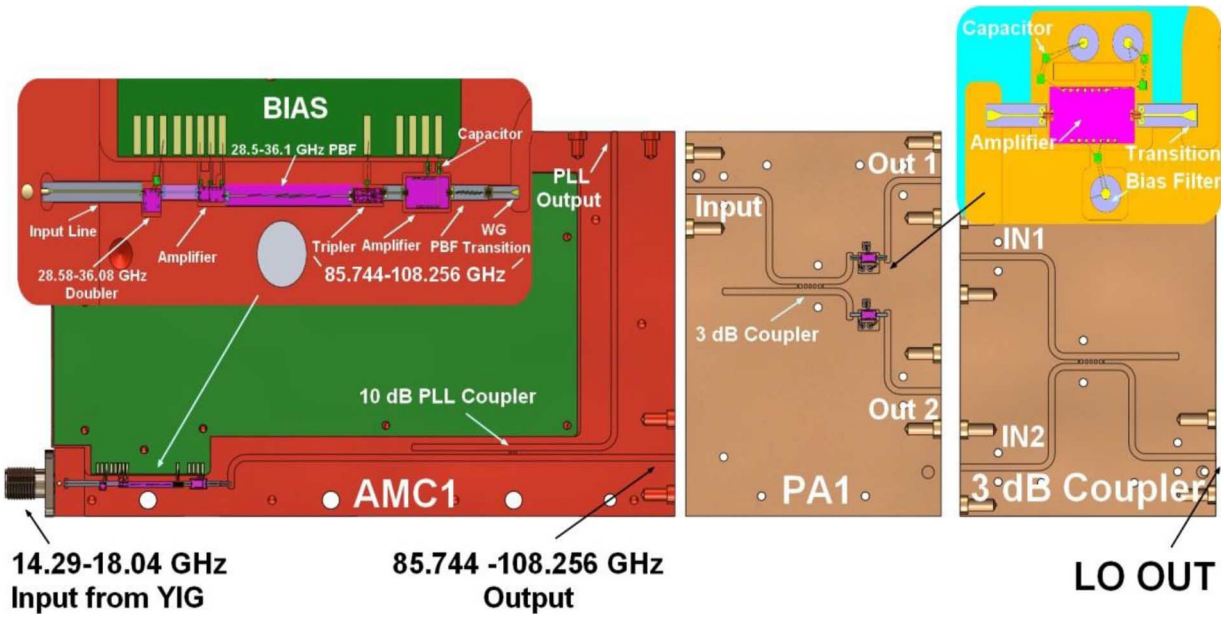

Fig. 2. AMC, PA, and 3-dB coupler which are parts of the NOEMA LO system. Design details of the multiplied chain microassembly of the AMC1, used in the NOEMA Band-1 LO, are shown on the inset on the top left. Details of the 3-mm band MMIC microassembly of the PA1, to be used in a future 3-mm multibeam receiver LO, is shown in the inset on the top right.

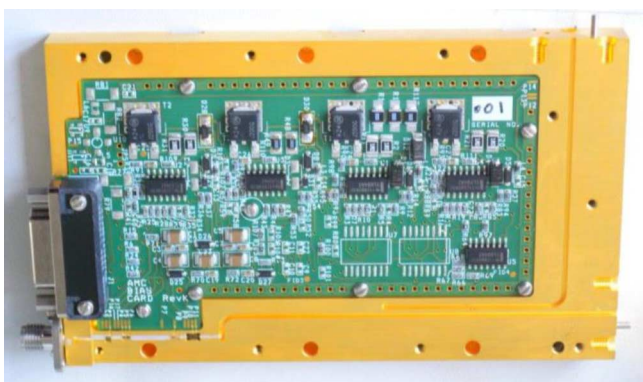

Fig. 3. AMC developed for the NOEMA LO Band-1 system (AMC1).

- The NOEMA PLL uses a mm-wave waveguide coupler inside the AMC with a coupling value of 10 dB (resulting in 10% coupling power losses) rather than 3 dB (resulting in 50% coupling power losses), as used in ALMA . Use of the 10-dB coupler increases the power level available at the AMC output.
- NOEMA uses an external harmonic mixer rather than a fundamental internal one, allowing us to adopt a first LO reference (REF1) between 13–16.4 GHz. A signal in this frequency range is easier to synthesize than the mm-wave REF1 signal used by ALMA in its PLL. An high rejection tubular filter and a low-noise amplifier are placed between the harmonic mixer and the PLL to minimize the noise bandwidth and improve the spurious harmonics rejection of the harmonic mixer with the 100-MHz IF. Such filter rejection would be difficult to obtain through an integrated filter, as used in ALMA.
- A different active doubler (HMC578), which operates at lower frequencies than the one used in ALMA Band 3 (CHX2091), is adopted [6] for the NOEMA Bands 1–3 LOs.

TABLE I
MMIC PROPERTIES

MMIC name	f_{min} (GHz)	f_{max} (GHz)	NOEMA Band
Ampli EBPA 75	60	87	2, 3
Ampli EBPA 96B	81	110	1
Ampli EBPA107C	92	122	4
Tripler 110TRP1	90	124	1, 4
Tripler 81TRP1	70	92	2, 3
Doubler HMC 578	24	33	1, 2, 3
Doubler CHX2091	32	40	4
Ampli AMMC5040	23	40	1, 2, 3, 4

TABLE II
YIG PROPERTIES

YIG Name	f_{min} (GHz)	f_{max} (GHz)	NOEMA Band
MLXS1783	12.86	19.53	1
MLXS1795	11	15	2, 3
MLOS 1604	15	21	4

B. Micro-Assembly and Couplers

We now describe the MMIC, filters, waveguide-to-microstrip transition, and waveguide coupler.

1) MMIC: Table I summarizes for each band the type, names, and frequency ranges of the MMICs that are integrated into the modules of AMCs and PAs. The EBPA amplifiers and the TRP triplers were designed by NRAO (see [3] and [9]). The other devices are commercially available. Table II shows, for each band, the name and the frequency ranges of the YIG oscillators.

2) Filter Design: The passband filters (PBFs) employed in the AMC modules (shown in Fig. 2) were designed with the commercial software ADS (Keysight Technologies). They

TABLE III
PASSBAND FILTER PROPERTIES

Band	*Frequency (GHz)*	*W1 (μm)*	*W2 (μm)*	*W3 (μm)*	*L1 (μm)*	L2 (μm)	*L3 (μm)*	*S1 (μm)*	*S2 (μm)*	*S3 (μm)*
1	*28-36.4*	*34*	*49*	*53*	*976*	922	*947*	*12*	*24*	*32*
1	*85-109*	*33*	*46*	*46*	*300*	292	*292*	*14*	*29*	*39*
2, 3	*21-31*	*20*	*31*	*44*	*1280*	1140	*1170*	*12*	*15*	*15*
2, 3	*66-90*	*33*	*34*	*33*	*366*	366	*368*	*14*	*29*	*39*
4	*31.4-40.2*	*34*	*49*	*53*	*815*	807	*805*	*12*	*24*	*32*
4	*91.3-121.7*	*36*	*54*	*60*	*257*	252	*251*	*14*	*29*	*39*

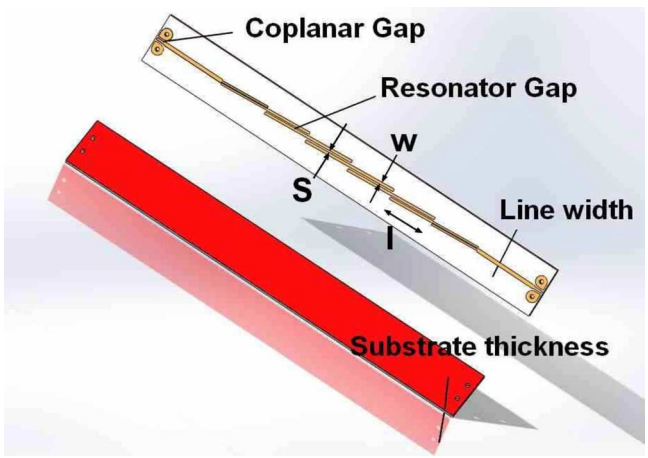

Fig. 4. Typical bandpass filter on alumina substrate showing the microstrip coupled lines and the nomenclature of the lines length (l), width (w), and gap (s). The filter backside (ground plane) is metalized (Au 2 μm). Parameter values are given in Table III.

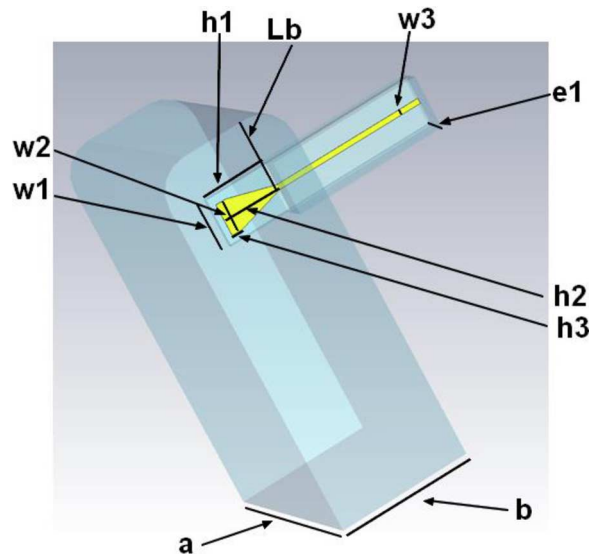

Fig. 5. View of the WR10 waveguide-to-microstrip transition with the model dimension parameters (parameters value given in Table IV).

consist of six pairs of microstrip coupled lines interfaced with coplanar lines at the filter input and output, as shown in Fig. 4. The three last filter sections are the mirror of the three first sections relative to the filter center. The lines are deposited on 80-μm-thick Al_2O_3-99.6% metalized substrate.[2] Table III shows for each band and the three first filter sections the values of the coupled lines length (l), width (w), and gap (s).

3) WR10 Waveguide-to-Microstrip Line Transition: Fig. 5 shows the details of the WR10 waveguide to microstrip line which was optimized with the solver CST Microwave studio.

The transition is deposed on an 80-μm-thick Al_2O_3-99.6% metalized substrate .

Table IV gives the optimized parameters of the transition: the WR10 waveguide width (a) and height (b), the substrate width (w1), the antenna width (w2), the line width (w3), the substrate height inside the waveguide (h1), the antenna height inside the waveguide (h2), the antenna rectangular height (h3), the substrate channel height (e1), and the distance between the waveguide short and the middle of the line (Lb). The antenna metalized surface plane is placed at the center of the WR10 waveguide width. The chip integrates at its output a microstrip-to-coplanar waveguide transition (not shown).

4) Coupler Design: The waveguide hybrid couplers (10-dB coupling, 90° phase difference) for the PLLs, which are part of the AMCs, consist of two $\lambda_g/4$ sections of branch-line waveguides. The waveguide hybrid couplers (3-dB coupling, 90° phase difference) of the PAs and 3-dB recombination modules consist of six sections of $\lambda_g/4$ waveguide branch-lines with variable width, as shown in Fig. 6. Table V shows for each band the coupling and the first branch-lines dimensions: the widths (ws), the pitch (ps), and length (ls). The couplers geometry is optimized using the commercial electromagnetic solvers ADS and CST Microwave Studio.

IV. LO FABRICATION

A. LO Rack

Fig. 7 shows one of the fully assembled LO racks for the NOEMA LO Band 4. The rack integrates the YIG oscillator, which is cascaded with an isolator and filter and screened with absorbers glued on the inner surfaces of a copper enclosure, the AMC, the PA, the 3-dB coupler, the CAN interface, the harmonic mixer, the filters, the amplifiers, as well as the coaxial connectors carrying the two reference signals. Fig. 8 shows four production series NOEMA Band-1 LO racks. DC biasing of the

[2][Online]. Available: http://www.thinfilm.com/

TABLE IV
WR10 WAVEGUIDE-TO-MICROSTRIP TRANSITION DIMENSIONS

a (mils)	*b* (mils)	*w1* (mils)	*w2* (mils)	*w3* (mils)	*h1* (mils)	*h2* (mils)	*h3* (mils)	*e1* (mils)	*Lb* (mils)
100	50	20	12	2	22	20	4	12	37

TABLE V
COUPLER PROPERTIES

Band Standard	*Coupling (dB)*	*Ws1 (mm)*	*Ws2 (mm)*	*Ws3 (mm)*	*ps1 (mm)*	*ps2 (mm)*	*ps3 (mm)*	*ls (mm)*
1, (WR10)	11	0.39	0.39	-	0.63	-	-	0.695
1, (WR10)	3	0.23	0.44	0.4	1.01	0.945	0.834	0.711
2,3, (WR12)	10	0.45	0.45	-	1.2	-	-	0.85
2, 3, (WR12)	3	0.29	0.55	0.49	1.25	1.17	1.03	0.85
4, (WR8)	10	0.33	0.33	-	0.98	-	-	0.76
4, (WR8)	3	0.21	0.31	0.30	0.98	0.85	0.76	0.75

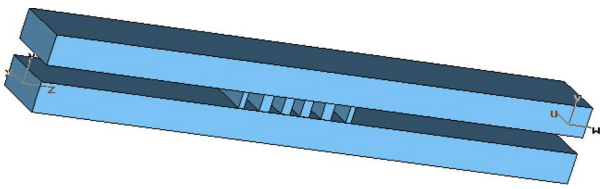

Fig. 6. Typical 3-dB-90° branch-line waveguide hybrid coupler with six $\lambda_g/4$ sections used in the mm-wave LO system. A waveguide load is integrated into the unused waveguide port (parameter values given in Table V).

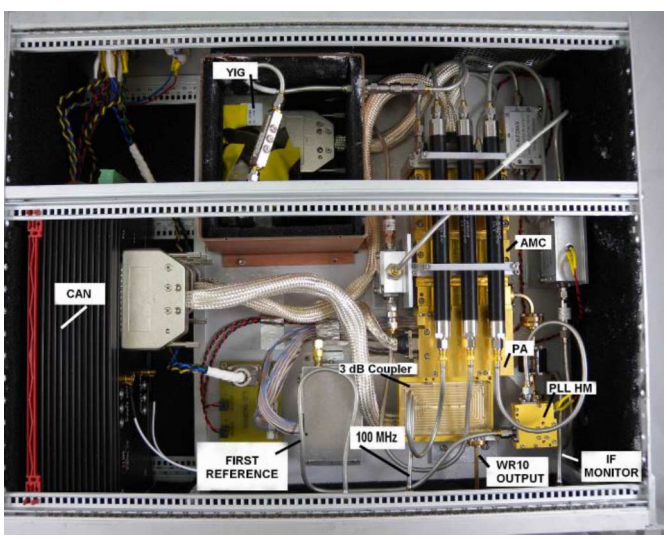

Fig. 7. NOEMA Band-4 LO rack showing the CAN remote control interfaces, the YIG oscillator, the AMC, PA, and 3-dB combination coupler, the PLL HM, the output WR8 waveguide flange.

(a) (b)

Fig. 8. (a) Four production series of NOEMA Band-1 (∼ 82–108.2 GHz) LO racks and (b) their power supply racks.

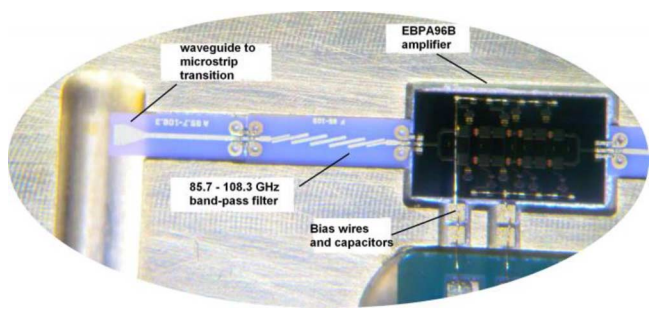

Fig. 9. Photograph showing part of the LO Band-1 AMC chain microassembly with transition from WR10 waveguide to microstrip, the 85.7–108.3-GHz band-pass filter, the EBPA96B amplifier, the signal coplanar ribbon, and the bonding wires for biasing the MMIC.

inner LO rack modules is provided by dedicated power supply racks.

B. LO Micro-Assembly

Fig. 9 shows a view of the microassembly around the final 3-mm band MMIC amplifier [3] located inside the LO Band-1 AMC chain. The MMIC amplifier is bonded at its output to the 85.7–108.3-GHz bandpass filter, which in turn is bonded to the waveguide-to-microstrip transition chip. Fig. 10 shows a photograph of the PA microassembly that divides over a 3-dB hybrid coupler the signal received from the AMC chain in two channels where the signal is amplified through two millimeter MMIC amplifiers.

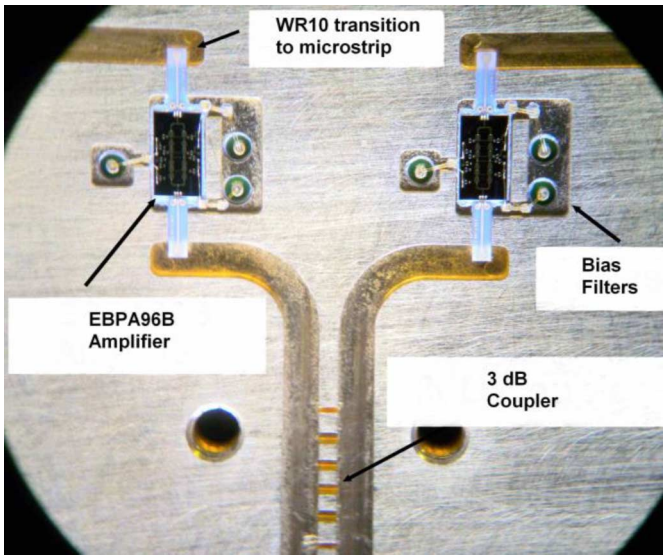

Fig. 10. Photograph showing part of the LO Band-1 PA with the 3-dB hybrid coupler, four transitions from WR10 waveguide to microstrip, two EBPA96B amplifiers, the signal coplanar ribbon, the bonding wires, and bias filters to bias the MMIC.

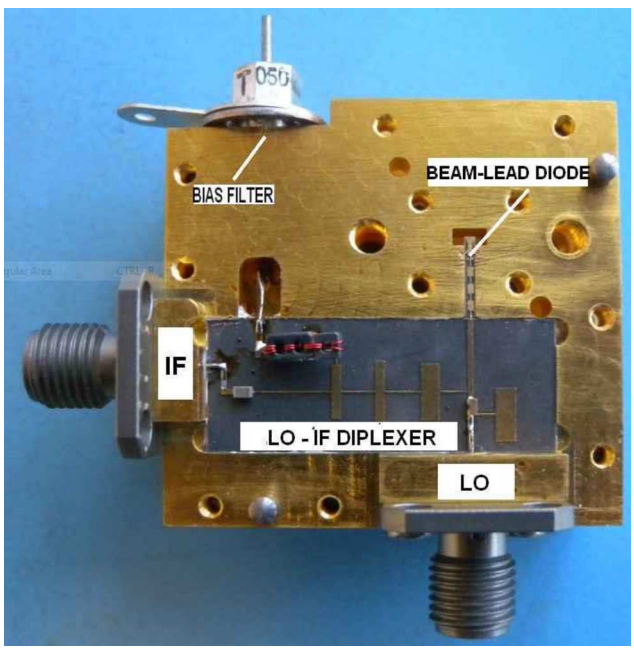

Fig. 11. View of the WR10 harmonic mixer used in the LO Band 1 with details of beam-lead diode, LO—IF diplexer and bias circuits.

C. LO PLL Harmonic Mixer

An harmonic mixer is employed in the PLL circuitry of the Band 1 LO. Its internal details are shown in Fig. 11. The harmonic mixer integrates a diplexer and employs a beam-lead.

Schottky diode coupled to a WR10 waveguide, an LO filter passing the band 13–40 GHz, an IF filter passing the band dc–4 GHz, and a bias filter. The RF circuits are metalized on a 5-mils-thick substrate (Duroid Rogers 5880).

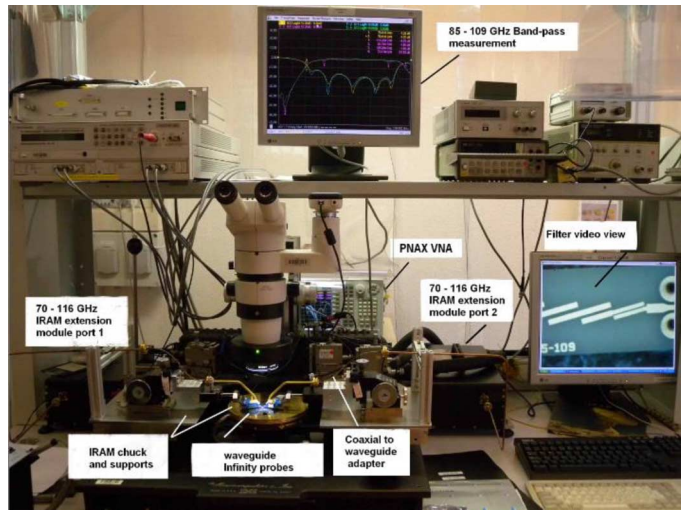

Fig. 12. In-house-made IRAM millimeter coplanar prober and MVNA measuring the transmission and reflexion responses of one AMC 85–109-GHz bandpass filter.

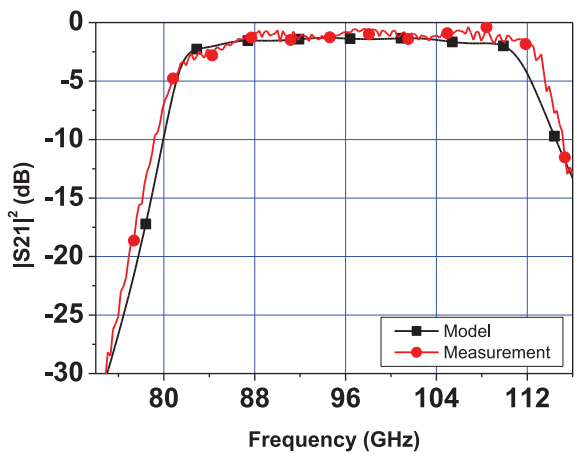

Fig. 13. Graph of the 85–109-GHz bandpass filter transmission with the measured (red circles) and modelled (black squares) responses.

V. LO Measurement Results

We summarize the main measurement results of the filters, of the couplers and of the harmonic mixers employed in the LO systems. Also, we present the results of the final LO systems, which include AMC and PA output powers and phase noise.

A. Filter Measurement

1) Setup: The responses of the bandpass filters, which are part of the AMC module, were measured using the IRAM built Millimeter-wave Vector Network Analyzer (MVNA). For the 85–109-GHz bandpass filter measurement, the MVNA is interfaced with a coplanar millimeter prober system, as shown Fig. 12.

2) Filter Response: Fig. 13 shows the measured and the simulated responses of the 85–109-GHz bandpass filter. A dielectric constant $\varepsilon_r = 9.4$ was used to design this filter. The dielectric constant was derived by extrapolating previous measurements of the Band4 LO bandpass filters, where the value was adjusted to best-fit the measured filter response. Instead, a dielectric constant of $\varepsilon_r = 9.9$ was used to design the 28-36.4-GHz bandpass

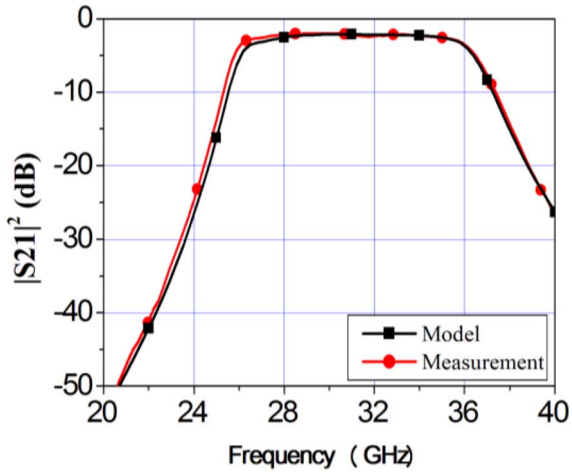

Fig. 14. Graph of the 28–36.4-GHz bandpass filter transmission with the measured (red circles) and modelled (black squares) responses.

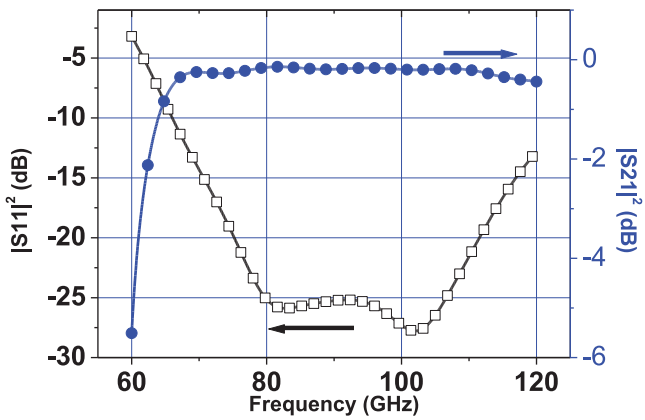

Fig. 15. Simulated reflection (left scale) and transmission (right scale) coefficients of the WR10 waveguide-to-microstrip line transmission of Fig. 4 (parameters given in Table IV).

filter (see dimensions in Table IV), whose response is shown in Fig. 14.

B. WR10 Waveguide-to-Microstrip Line Transition Model Response

The simulated results of the 3-D electromagnetic simulation (with the commercial software CST) of the WR10 waveguide-to-microstrip line transition of Fig. 4 are shown in Fig. 15. We did not measure this transition.

C. Coupler Response

The measured and simulated responses of the WR10 3 dB hybrid coupler of the LO Band 1 (Fig. 6, Table V) are shown in Fig. 16. The 3-D electromagnetic model was limited to the branch lines part to reduce the simulation time. The slight difference of $\sim$ 0.3 dB between the model and the measured curves of S-parameters results from the waveguide propagation losses that were not included in the model.

D. Harmonic Mixer Measurement

The conversion losses of the WR10 LO Band-1 PLL harmonic mixer shown in Fig. 11 were measured using the first reference LO (13–16.4 GHz). The power of the RF signal was

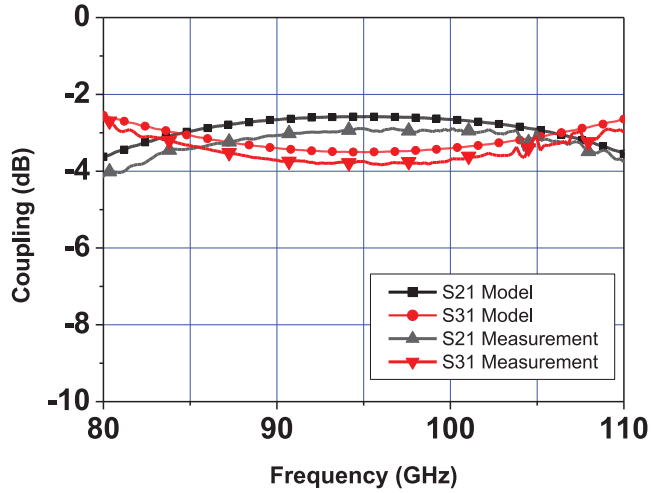

Fig. 16. Graph of the measured and modelled coupling for the LO Band-1 WR10 3-dB coupler.

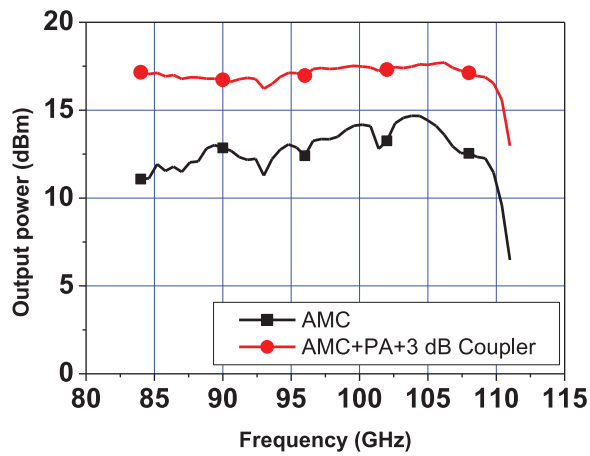

Fig. 17. Measured output power of the LO Band-1 AMC chain (black squares) and AMC + PA + 3 dB coupler (red circles).

measured with a WR10 power-meter. The IF signal at a frequency of 100 MHz was obtained from the mixing of the RF signal and the seventh-harmonic of the first reference LO. The measured conversion losses, given by the ratio of the IF level over the RF level, were between 20 and 25 dB over the full LO band.

E. Output Power

The curves in Fig. 17 show the output powers measured at the output waveguide flange of the LO Band 1 rack equipped with AMC + PA + 3 dB coupler, of order +17 Dbm, and equipped with AMC only, of order +13 dBm. The output power largely exceeds the requirements for optimum pumping of the 3-mm band NOEMA 2SB SIS receiver, therefore a 15-dB attenuator needs to be cascaded with the AMC chain in order to bring the LO Band-1 output power within a suitable range.

The measured output power of the eight 3 mm band modules (94.3–121.6 GHz) employed in the Band-4 LO systems (283–365 GHz) is shown in Fig. 18. The power difference between the LOs comes from the performances dispersion of the MMICs used in the chain and from the accuracy of the

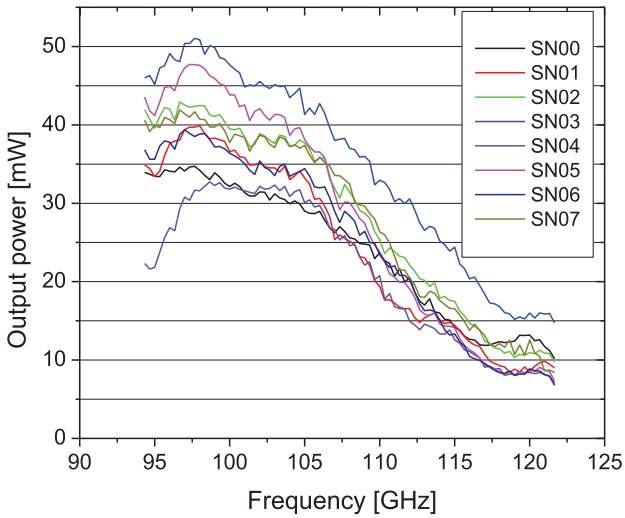

Fig. 18. Measured output power of eight 3-mm band modules (94.3–121.6 GHz) produced for the LO Band-4 system.

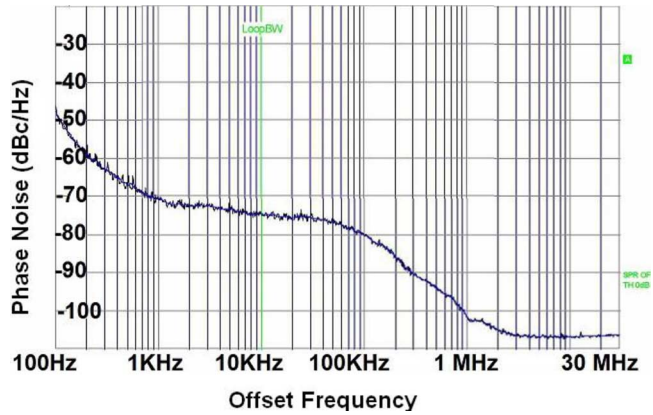

Fig. 19. LO Band-4 spectral phase noise density measured at 325 GHz with an R&S FSUP signal analyzer. Horizontal axis: logarithmic scale between 100 Hz to 30 MHz, Vertical axis: linear scale between −20 dBc/Hz to −110 dBc/Hz–10 dB/div.

micro-assembly process. The LO output power is adjusted by changing the drain voltage of the MMIC amplifiers located in the AMC and the PA. The power was tuned between 5 μW and the maximum output power shown in Fig. 18. The YIG-based LO system allows us to phase-lock on a time scale of the order of only a few seconds, as is required to execute a program code interfaced with an electronically tuned LO. Such a phase-lock time is much shorter than the time required to lock the mechanically tuned Gunn oscillators (of the order of several minutes, for program codes interfaced with mechanically tuned backshorts). The Band-4 LO was successfully installed on the PdBI antennas and the first astronomical observations were performed across Band 4 in late 2010, thus opening up the sub-mm-wave window at the PdBI observatory. This was the first time that a YIG-based Local Oscillator was used at the IRAM observatories.

F. LO Phase Noise

The phase noise was measured at the output of the Band 4 LO that consists of an active multiplied chain (AMC + PA + 3-dB coupler) followed by a VDI WR2.8×3 frequency tripler . The measurement was made directly at 325 GHz using an external WR3 harmonic mixer developed at IRAM, which down-converts the LO signal across the input RF band of a FSUP26 signal source analyzer.[3] The Band-4 LO was locked following the method shown in Fig. 1 and described in Section II. The REF1 reference signal is generated by a YIG oscillator whose PLL first reference is another signal at 1.8 GHz generated by a Rohde&Schwarz SMA 100 synthesizer. Fig. 19 shows the LO phase noise spectral density measured at 325 GHz. The integration between 100 Hz and 30 MHz of the noise spectral density gives a phase noise of $\sim$ 5° rms. Such phase noise results in a loss of interferometric efficiency between two antennas of less than 0.76% [8]. This is within the specification, as the maximum admissible degradation of the NOEMA interferometer efficiency caused by the LO phase noise is 1%. When the YIG is locked, the LO stability equals the stability of the signal references. The reference of the interferometer is a 5 MHz maser source with stability of $7 \cdot 10^{-14}/\mathrm{s}$. The first reference (REF1) and second reference (REF2) are both synchronized to the 5-MHz maser reference.

[3][Online]. Available: http://www.rohde-schwarz.com

VI. LO Spurious Harmonics and Filtering

The multiplied chain of the LO system uses active and passive multipliers that, in addition to the main (wanted) LO tone, might be source of unwanted harmonics at the SIS mixer LO input. Thus, an unwanted down-conversion might result from a beating of the LO harmonic frequencies and the frequencies of the astronomical sources if their frequency difference falls into the IF band. This can lead to spurious detection of astronomical lines whose frequencies are outside the nominal RF band as long as the SIS mixer is able to respond to those frequencies ("ghost lines" [7]). Also, the SIS mixer can act as multiplier of the LO frequencies, thus generating unwanted harmonics. Whatever the harmonic generation mechanism, if the power of these harmonics is high enough (compared to the fundamental tone) to sufficiently pump the SIS mixer, it can increase the SIS receiver noise temperature by adding noise from the sidebands of the harmonics to the IF output.

The tones can also have sufficient pumping power to produce a detection of unwanted spectral lines on the sidebands of the LO spurious signal during astronomy observations.

As an example, we have detected, in the setup of Fig. 20, the LO spurious harmonics present in the signal of a Band-2 Gunn LO system consisting of a $\sim$ 67–90-GHz Gunn (itself working in second harmonic) followed by a VDI frequency doubler. The LO system is expected to deliver a final LO signal with a main tone tunable across $\sim$ 134–180 GHz. RF signals of frequency near the third harmonic (H3), the fourth harmonic (H4), and the fifth harmonic (H5) of the $\sim$ 67–90-GHz Gunn oscillator were injected, in turn, through the receiver RF input in order to produce a beat with the spurious harmonics of the LO doubler; these would result in a line detection, measured using a spectrum analyzer, in the 2SB receiver IF bands, either LSB, USB or both. The injected RF power level at the receiver input was not precisely known, but it was fixed at a level that did not induce

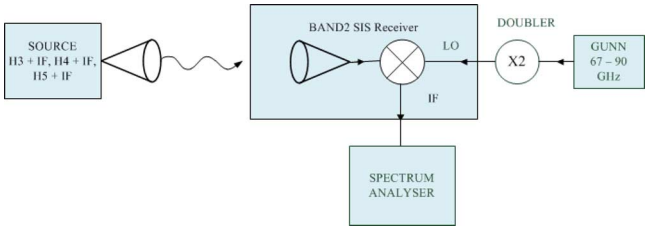

Fig. 20. Band-2 LO harmonics measurement setup.

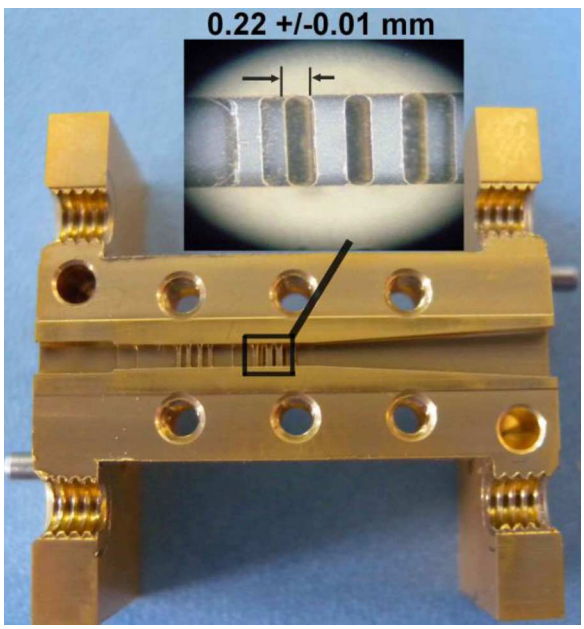

Fig. 21. LO band 2 134–184-GHz bandpass filter showing the detail of the machining precision, the WR6 input waveguide and the WR10 output waveguide. WR10 is the waveguide standard of the over-moded LO waveguide at the cryostat input.

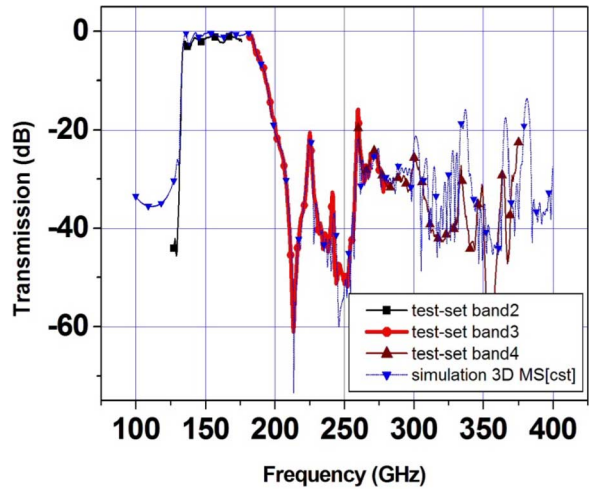

Fig. 22. LO band 2 134–184-GHz bandpass filter response measured and modelled over the 100–375-GHz band.

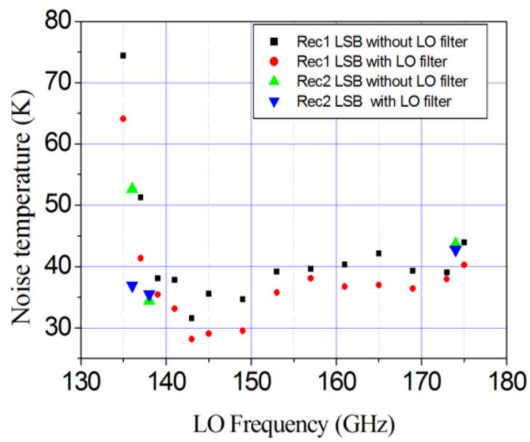

Fig. 23. Noise temperatures of two Band-2 SIS receivers (LSB channel) measured with and without the cutoff filter at the output of the doubler of the Band 2 electronically tuned YIG LO. The receiver noise temperature is strongly reduced between 136 and 138 GHz when the filter is used.

any junction current through the SIS mixer, in order to avoid a pumping effect by the RF injected signal.

To mitigate the LO spurious harmonics problem, we designed, fabricated and characterized a $\sim$ 134–184-GHz bandpass filter (see Fig. 21). The filter reduces the power of the third and fourth harmonics (H3 and H4) as well as part of the fifth harmonic (H5) at the output of the VDI frequency doubler. Up to a frequency of 132 GHz, the filter also reduces the power magnitude of the H3 from the fundamental frequency of the harmonic-2 Gunn oscillator, which pumps the Band-2 LO doubler. Fig. 22 shows the measured and modelled responses of the 134–184-GHz bandpass filter. The filter measurements were made using three of the IRAM VNA mm-wave extension heads, namely the Bands 2–4 IRAM MVNA test-sets. For frequencies up to $\sim$ 300 GHz the measurements are in close agreement with the model, even for very low transmission levels (-50 dB).

With the level of the doubler H3 reduced by more than 20 dB using the bandpass filter, the receiver noise temperature for an LO tuning at 136 GHz decreased by $\sim$ 16 K in the LSB and by 11 K in the USB (in particular, the measured receiver noise was reduced from $\sim$ 53 K to $\sim$ 37 K in LSB). Fig. 23 shows for two receivers (Rec1&Rec2) the reduction of the LSB noise temperature when using the LO filter, which is stronger in the lower part of the band. The two receivers use two different LOs with different doublers. The receiver noise is less affected by the presence of the filter in the LO path for LO frequencies above 138 GHz because the power level of the external doubler third harmonic is probably too low to pump the SIS mixer. The receiver noise temperature was measured at these LO frequencies after a ghost line was detected at the 30-m Pico Veleta telescope using a Band-2 SIS receiver tuned at 136.42-GHz LO frequency. Such receivers use the same type of Gunn local oscillator followed by a VDI doubler as previously described. Ghost lines were not observed at the telescope above 138 GHz. After the LO filter was inserted in the 30-m telescope LO chain ahead of the VDI doubler, the ghost line problem was solved [7].

Although the bandpass filter reduced the H3, H4, H5 by more than 20 dB, there remains a signal detected across the IF band at the frequency of the theoretical H4 frequency. Using a WR3 cutoff waveguide placed at the doubler output, that cuts the LO fundamental frequency, but not H3, H4 and H5, the IF from the

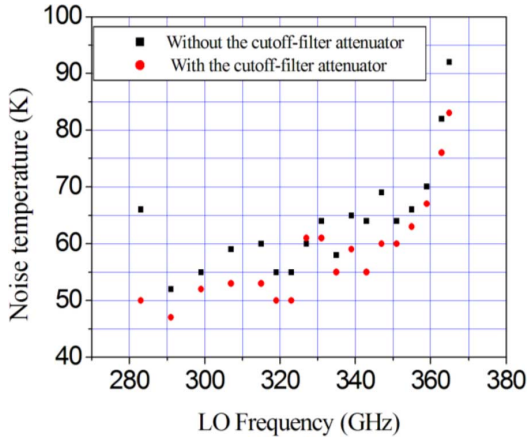

Fig. 24. Noise temperatures of a Band-4 SIS receiver measured with and without the cutoff filter at the tripler output of the Band-4 electronically tuned YIG LO.

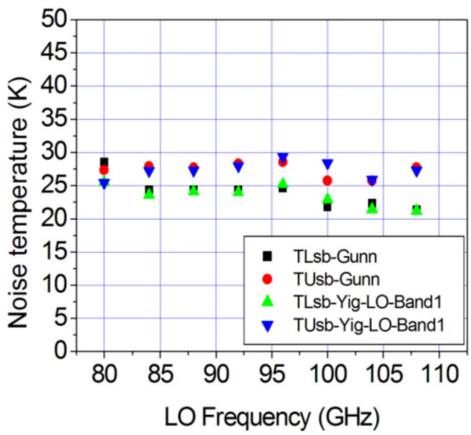

Fig. 25. Comparison of measured noise temperatures (LSB and USB) of a Band-1 SIS receiver pumped with a Gunn LO and with the developed Band-1 electronically tuned YIG LO.

H4 signal was dramatically reduced or even completely suppressed. This measurement shows that the largest contribution to the detected H4 signal magnitude comes from the second harmonic (H2) of the Band-2 LO frequency which is multiplied by the SIS mixer nonlinearity.

A similar approach is used to mitigate the spurious harmonics in other NOEMA LO bands: a stainless steel cutoff attenuator suppresses the SIS mixer noise excess caused by the H2 generated by the Band-4 LO output tripler, while a 15 dB attenuator located at the LO output is used to suppress the noise excess added to the Band-1 2SB SIS mixer, thus reducing together the signal and the noise level when high values of amplifier drain voltages are used. No problem of spurious harmonics is associated with the AMC1 integrated tripler. All spurious harmonics, including H2, are very well filtered by the 85–109-GHz bandpass filter that was specifically designed for this purpose. For an LO frequency of 108 GHz ($2 \times 3 \times 18$ GHz), the harmonic 2 at 72 GHz ($2 \times 2 \times 18$ GHz) is rejected by over 30 dB. The excess noise temperature caused by the Band 4 LO output tripler second harmonic was reduced by 15 K using the cut-off attenuator at the tripler output. The effect of the filter on the Band-4 LO chain is also important on the lower part of the band because the tripler H2 magnitude decreases with frequency (Fig. 24). Using a 15-dB attenuator at the Band-1 LO AMC output, there is no LO excess noise on the SIS mixer given by the electronically tuned Band-1 LO compared with a Gunn oscillator LO. Fig. 25 shows the measurements, carried out across the 80–108-GHz LO band (72–116 GHz RF frequency), of the USB and LSB noise temperatures of a Band-1 SIS receiver pumped with a Gunn LO and with the electronically tuned Band 1 LO. As can be seen, there is no significant difference in noise between the two sources. The LO frequency band covered is 28 GHz, i.e., 30% of the central LO frequency (94 GHz). This represents an important improvement over the frequency band covered by the 92–108-GHz Band-3 AMC3 of ALMA (16% of the 100-GHz central frequency).

VII. Conclusion

We presented the LO system developed for the NOEMA project and gave some details of its design. Eight Band-4 and five Band-1 LO racks were successfully produced. The output power of the Band-4 LO is between +13 and +18 dBm across the $\sim$ 93–121-GHz band using an AMC followed by a PA and 3-dB coupler modules. The NOEMA LO Band-1 employs only an AMC chain delivering between $\sim$ +11 and +15 dBm in the 82–109-GHz band. Across the LO Band 1, the power is between $\sim$ +16 and +18 dBm when adding a PA and 3-dB module in cascade to the AMC chain; such a configuration can be used for a multibeam receiver LO.

The generation of spurious harmonics along the local oscillator chain was discussed and a solution was implemented that strongly mitigates the problem by filtering was presented.

The main differences of our NOEMA LO with respect to the ALMA LO were described. The NOEMA Band-1 LO has 30% fractional bandwidth, which considerably improved the fractional band of the AMC of ALMA Band 3 (of $\sim$ 16%).

Acknowledgment

The authors would like to thank M. Berton for assistance with the fabrication of the harmonic mixers bias card, J. M. Dannell for the machining of the AMC blocks and 3-dB couplers prototypes, and J. Reverdy for his help during the measurements of the Band-2 LO harmonics and the SIS receiver noise temperature.

References

[1] J. E. Carlstrom, R. L. Plambeck, and D. D. Thornton, "A continuously tunable 65–115 GHz Gunn oscillator," *IEEE Trans. Microw. Theory Techn.*, vol. 33, no. 7, pp. 610–619, Jul. 1985.

[2] E. Bryerton, K. Saini, M. Morgan, M. Stogoski, T. Boyd, and D. Thacker, "Development of electronically tuned local oscillators for ALMA," in *Proc. 30th Int Conf on IR and MM Waves and 13th Int. Conf. on THz Electron.*, Williamsburg, VA, USA, Sep. 19–23, 2005, vol. 1, pp. 72–73.

[3] M. Morgan *et al.*, "Wideband medium power amplifiers using a short gate-length gaas MMIC processs," in *IEEE MTT-S Int. Microw. Symp. Dig.*, Boston, MA, Jun. 2009, pp. 541–544.

[4] F. Mattiocco *et al.*, "Electronically tuned local oscillator for the NOEMA interferometer," in *Proc. 26th Int. Symp. Space THz Technol.*, Cambridge, MA, USA, Mar. 16–18, 2015, p. paper P-29.

[5] *46515 Landing Parkway Fremont, 94538.* , CA, United States: Micro Lambda Wireless, Inc.

[6] J. Y. Chenu *et al.*, "Design of the front-end for the NOEMA interferometer," in *Proc. 23th Int. Symp. Space THz Technol.*, Groningen, The Netherlands, Apr. 8–10, 2013, paper M3–2.

[7] A. Sievers, D. John, S. Navarro, and C. Kramer, "Work report on ghost line observations with E150 on IRC+10216 of 11-March-2015 IRAM Internal Report, V1.2," Pico Veleta, Spain, 2015.
[8] A. R. Thomson, J. M. Moran, and G. W. Swenson Jr, *Interferometry and Synthesis in Radio Astronomy*. Hoboken, NJ, USA: Wiley, 2001, p. 429.
[9] M. Morgan, "Millimeter-wave MMICs and Applications," Ph.D. dissertation, Dept. Submillimeter Wave Astrophys., Cal. Inst. Technol., Pasadena, CA, USA, 2003.

Francois Mattiocco (M'09) received the M.S. and Ph.D. degrees in electronic, instrumentation, and metrology from the University of Pierre & Marie Curie, Paris, France, in 1976 and 1979, respectively.

From 1980 to 1984, he was with Thomson CSF, where he was involved with the development of parametric amplifiers for satellite communications. Since 1984, he has been in the Receiver Group of the Institut de RadioAstronomie Millimétrique (IRAM), Saint Martin d'Hères, France, where he was involved in the development of millimeter devices and systems (e.g., Gunn oscillators, multipliers, harmonic mixers, centimeter radiometers for antenna holography and interferometric atmospheric phase correction). His research interest has included the development of a novel submillimeter vector network analyzer. Now his work focuses on wideband electronically tuned millimeter local oscillators for SIS receivers used in radio astronomy.

Olivier Garnier received the three-year university degree in electronics from Institut Universitaire de Technologie, Salon-de-Provence, France.

He joined the Institut de Radioastronomie Millimétrique (IRAM), Saint Martin d'Hères, France, in 2006, where he is currently working on assembly and characterization of millimeter-wave components and front-ends.

Doris Maier received the S.M. and Ph.D. degrees in physics from the University of Cologne, Cologne, Germany, in 1993 and 1996, respectively.

She is currently with the Institut de Radioastronomie Millimétrique (IRAM), Saint Martin d'`Hères, France, where she is working on the development of submillimeter-wave instrumentation for radio astronomy.

Alessandro Navarrini received the S.M. degree in physics from the University of Florence, Florence, Italy, in 1996, and the Ph.D. degree in electronics and microelectronics from the Université Joseph Fourier, Saint Martin d'Hères, France, in 2002.

From 1998 to 2003, he was with the Institut de Radioastronomie Millimétrique (IRAM), Saint Martin d'Hères, France, where he was involved in the development of low-noise superconducting SIS receivers. From 2003 to 2006, he was a Post-Doctoral Fellow with the Radio Astronomy Laboratory, University of California, Berkeley, CA, USA. In 2006, he joined the National Institute for Astrophysics (INAF), Cagliari Astronomy Observatory, Capoterra, Italy. From 2010 to 2015, he was with IRAM, Saint Martin d'Hères, France, where he was in charge of the Front-End Group. Since 2015, he has been with the National Institute for Astrophysics (INAF), Radio Astronomy Observatory, Cagliari, Italy. His research interests include radio astronomy instrumentation and in particular low-noise microwave and millimeter-wave receivers.

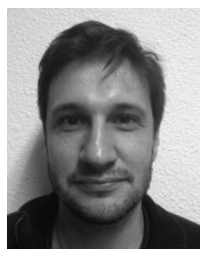

Patrice Serres received the S.M. degree in microelectronics and microwaves from the Sciences and Technologies University of Lille, Lille, France, in 2002.

Since 2002, he has been with the Institut de Radioastronomie Millimétrique (IRAM), Saint Martin d'Hères, France, where he is involved in the development of cryogenic low noise millimeter wave receivers. His work focuses particularly on SIS mixer development and on cryogenic low-noise HEMT amplifier integration and tests.